

Learning-based Autonomous Oversteer Control and Collision Avoidance

Seokjun Lee and Seung-Hyun Kong*, *Senior Member, IEEE*

Abstract—Oversteer, wherein a vehicle’s rear tires lose traction and induce unintentional excessive yaw, poses critical safety challenges. Failing to control oversteer often leads to severe traffic accidents. Although recent autonomous driving efforts have attempted to handle oversteer through stabilizing maneuvers, the majority rely on expert-defined trajectories or assume obstacle-free environments, limiting real-world applicability. This paper introduces a novel end-to-end (E2E) autonomous driving approach that tackles oversteer control and collision avoidance simultaneously. Existing E2E techniques, including Imitation Learning (IL), Reinforcement Learning (RL), and Hybrid Learning (HL), generally require near-optimal demonstrations or extensive experience. Yet even skilled human drivers struggle to provide perfect demonstrations under oversteer, and high transition variance hinders accumulating sufficient data. Hence, we present Q-Compared Soft Actor-Critic (QC-SAC), a new HL algorithm that effectively learns from suboptimal demonstration data and adapts rapidly to new conditions. To evaluate QC-SAC, we introduce a benchmark inspired by real-world driver training: a vehicle encounters sudden oversteer on a slippery surface and must avoid randomly placed obstacles ahead. Experimental results show QC-SAC attains near-optimal driving policies, significantly surpassing state-of-the-art IL, RL, and HL baselines. Our method demonstrates the world’s first safe autonomous oversteer control with obstacle avoidance.

Index Terms—Autonomous driving, oversteer, collision avoidance, imitation learning, reinforcement learning

I. INTRODUCTION

WHEN slip occurs between a vehicle’s tires and the road surface, causing the tires to skid, the vehicle becomes highly unstable. Particularly, when the rear tires lose traction, the vehicle rotates more than the driver intends and heads in an unintended direction; this phenomenon is known as oversteer (Refer to Fig.1a). Oversteer primarily occurs due to causes such as reduced road friction caused by road icing or hydroplaning, tire slippage from sharp steering or pedal manipulation beyond the vehicle’s limits, or rear-end collisions. Controlling oversteer requires both appropriate pedal manipulation and adequate counter-steering (a sophisticated driving technique where the driver steers in the opposite direction of the skid) at the same time [1]. However, it is very difficult for untrained ordinary drivers to use such a specialized driving technique. As a result, oversteer often leads to severe traffic accidents; according to the National Highway Traffic Safety Administration (NHTSA) Fatality Analysis Reporting System (FARS), oversteer accounted for more than 18,852

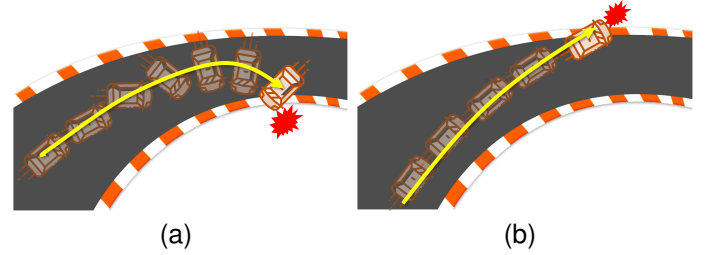


Fig. 1. Vehicle oversteer and understeer. (a) Oversteer: the rear tires lose the grip, and the vehicle rotates more than intended. (b) Understeer: the front tires lose the grip, and the vehicle turns less than expected.

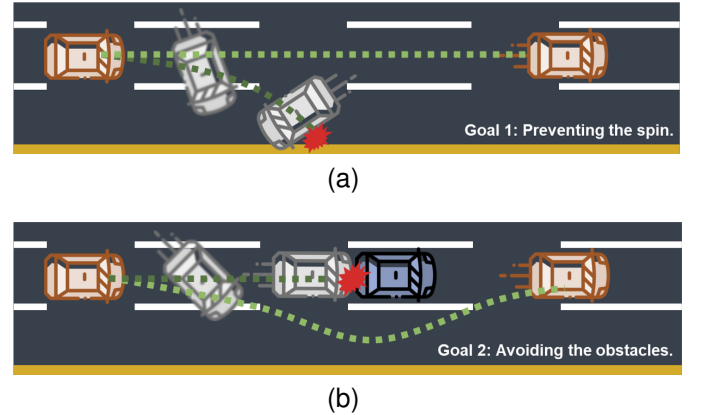


Fig. 2. Research goals. (a) Ego vehicle in brown must control the oversteer in order not to spin. (b) It should also avoid the obstacle (i.e., front vehicle) in blue.

fatal accidents in the United States from 2011 to 2020, making it the 8th leading cause of fatal accidents.

To mitigate oversteer, various methods have been proposed over the years. One of the earliest and most prevalent solutions is the implementation of Electronic Stability Control (ESC), which is now standard equipment in most modern vehicles. ESC helps prevent vehicle skidding by braking individual wheels or cutting engine power. However, it can only lower the slip probability but not eliminate it entirely [2]. Moreover, since ESC adjusts wheel forces rather than steering inputs, it lacks the ability to return a vehicle that has already entered an oversteer condition back to a stable, grip state. To address the limitations of ESC, researchers have explored autonomous driving technologies that enable automatic counter-steering, allowing vehicles to correct oversteer without driver intervention. Most of these technologies focus on control techniques designed to track predefined paths even under oversteer conditions [3]–[9]. While such methods can

*Corresponding author (email: skong@kaist.ac.kr)

Seokjun Lee and Seung-Hyun Kong are with the CCS Graduate School of Mobility, Korea Advanced Institute of Science and Technology, Daejeon, Korea, 34051 (email: {seokjunlee, skong}@kaist.ac.kr)

help an oversteering vehicle return to its original lane as shown in Fig.2a, they may not be sufficient in real-world scenarios where surrounding obstacles (e.g., other vehicles) are present. In these situations, merely controlling the oversteer is not enough to avoid collisions. When there is an obstacle in the driving lane, as illustrated in Fig.2b, the vehicle must not only regain stability but also recognize the surrounding environment and execute an evasive maneuver that ensures collision avoidance and is feasible for an oversteering vehicle to perform. To tackle this challenge, our study adopts an end-to-end (E2E) approach that directly maps the vehicle's state and surrounding environment to control actions by integrating path planning and vehicle control into a single neural network. This means that the path planning process simultaneously considers the vehicle's controllability, enabling the generation of paths that are both safe and executable under oversteer conditions.

In the realm of E2E autonomous driving, imitation learning (IL) and reinforcement learning (RL) have emerged as prominent techniques for training neural networks to perform complex driving tasks [10]–[15]. IL involves learning control policies by mimicking expert demonstrations, and RL enables an agent to learn optimal policies through trial-and-error interactions with the environment, guided by a reward function. However, both IL and RL have fundamental limitations. The action policies trained via IL often face significant performance degradation when they encounter novel situations where expert demonstration data is scarce or when the quality of the demonstration data is poor. On the other hand, even though RL requires sufficient experience of successful episodes, as the task becomes more complex, the state and action spaces become broader, and the transition dynamics have higher variance, the probability of experiencing successful episodes through random actions diminishes. Consequently, developing an optimal action policy using RL becomes exceedingly difficult [16], [17]. To overcome these shortcomings, recent hybrid learning (HL) techniques combine IL and RL, utilizing expert demonstration data with RL for more efficient and improved policy development [18]–[23]. However, HL techniques have a limitation in that the expert demonstrations must be nearly optimal or, even if noisy, must contain optimal demonstration data [23].

Such limitations in IL, RL, and HL become more critical when it comes to the vehicle oversteer situation. Firstly, it is nearly impossible under the oversteer situation to collect optimal demonstration data, because even human drivers find it difficult to react appropriately and try immature vehicle control. As a result, the driving policy trained via IL or HL techniques could perform poorly. Moreover, while controlling the oversteer and avoid nearby obstacles, there is an extensive amount of information to be perceived regarding the surroundings and the vehicle state, and there is a high transition variance due to the nonlinear dynamics. Not only does this make it challenging to develop an optimal driving policy using RL alone, but it also means that agents are unlikely to encounter the same situation multiple times, making it difficult to learn through repeated experiences. Therefore, there is a critical need for methods that enable fast learning from

new situations and can rapidly incorporate new successful experiences into the learning process.

To overcome the aforementioned limitations, we propose an innovative HL technique, Q-Compared Soft Actor-Critic (QC-SAC), capable of learning optimal policies even from immature demonstration data and adapting swiftly to novel situations. Using the proposed QC-SAC, we trained an autonomous driving agent capable of oversteer control and collision avoidance. In scenarios where even human drivers often fail to control the vehicle, a test vehicle equipped with the driving policy developed by QC-SAC successfully avoids obstacles when it suddenly starts to spin (oversteer) on a slippery road.

The major contributions of the paper are as follows:

- We introduce the world's first safe driving technology capable of successful autonomous control of vehicles that must avoid obstacles ahead while in an oversteer condition.
- We propose the first benchmark for training and evaluating autonomous driving agents capable of oversteer control and collision avoidance, inspired by the actual driver training process.
- We present a novel HL technique, QC-SAC, that effectively utilize immature demonstration data and adapt swiftly to novel situations. We also demonstrate the superior performance of QC-SAC in the proposed benchmark.

The remainder of this paper is organized as follows. Section II reviews prior works on autonomous oversteer control, and the representative learning techniques of E2E autonomous driving, which are IL, RL, and HL. Section III introduces the proposed Q-Compared Soft Actor-Critic (QC-SAC) algorithm and section IV describes the benchmark setup, and the state space, action space, and reward function used for the training of QC-SAC. Section V presents the experimental results and analysis, demonstrating the effectiveness of QC-SAC compared to baseline methods. Finally, section VI concludes the paper.

II. PRIOR WORKS

A. Autonomous Oversteer Control

Oversteer is a hazardous condition that poses significant challenges for vehicle stability control. Early approaches, such as Electronic Stability Control (ESC), aimed to prevent oversteer by modulating wheel forces (e.g., through selective braking or engine power reduction). While ESC effectively reduces the likelihood of slip, its reliance on wheel-force adjustments alone without direct steering interventions limits its ability to re-stabilize a vehicle already in an oversteer state. With the development of advanced steering actuation technologies, such as electronic power steering (EPS) and active front steering (AFS), it has become feasible to autonomously apply corrective steering inputs. This capability has prompted research into autonomous counter-steering methods specifically designed to address oversteer. Several studies have attempted oversteer control based on vehicle dynamics modeling [3]–[6], [24]. While vehicle dynamics models can be effective, they require extensive parameter measurements

beforehand and are susceptible to model mismatches due to various external factors. For instance, the widely used Pacejka Magic Formula [25], which models the nonlinear relationship between slip angle and tire force, relies on four parameters that must be measured in advance. These parameters are highly sensitive to external conditions like road surfaces, weather, tire temperature, and air pressure [26], making accurate modeling challenging. Acknowledging the limitations of dynamics-based methods, learning-based control approaches have been explored. Acosta *et al.* [7] proposed using neural networks to learn tire parameters for model-based controllers, while Cai *et al.* [8] and Cutler *et al.* [9] introduced reinforcement learning methods for drift control. However, both dynamics-based and learning-based methods have primarily targeted race-oriented scenarios, such as high-speed cornering or drift demonstrations, rather than focusing on traffic safety. As a result, these technologies often concentrate on tracking predefined trajectories or executing drifting maneuvers, while neglecting comprehensive path planning that includes obstacle avoidance. To our knowledge, all prior works either follow predefined expert trajectories [3]–[9] or perform simple path optimization in obstacle-free environments [5], [24].

However, on real roads with surrounding obstacles, simply following a predefined expert trajectory or conducting path optimization in an obstacle-free scenario is insufficient for safe evasive maneuvers under oversteer condition. An appropriate evasive path that can guarantee the safety and control feasibility is required. However, without an accurate vehicle model due to the uncertainty in the slip condition as mentioned earlier, it is extremely difficult to predict the future states and optimize the trajectory. If the planned path is not dynamically feasible, the vehicle may fail to avoid obstacles or even exacerbate the unstable behavior (e.g., reverse-steer¹) and increase the risk of collisions. These limitations highlight the necessity of tightly integrating path planning and control. Rather than decoupling these tasks, first planning a route and then attempting to trace it, our study embraces an end-to-end (E2E) approach. By mapping directly from the vehicle's current state and environmental observations to control actions, the E2E approach naturally ensures that generated paths are not only safe but also feasible under oversteer conditions. This approach alleviates the dependence on highly accurate predictive models, mitigates the risk of executing infeasible maneuvers, and provides a unified solution that simultaneously considers vehicle dynamics, environmental constraints, and the need for evasive, stability-preserving trajectories.

B. Imitation Learning (IL), Reinforcement Learning (RL), and the Hybrid Learning (HL)

In the field of E2E autonomous driving, two major methodologies have been widely explored: IL and RL [10]–[13]. Also, HL combining the advantages of IL and RL are being explored recently. In this section, we introduce the fundamental concept of IL, RL, and HL.

Firstly, IL is a form of supervised learning that aims to imitate the actions of an expert. The objective of IL is generally expressed as follows:

$$\arg \min_{\phi} \mathbb{E}_{(s_E, a_E) \sim \mathcal{D}} [\mathcal{L}(\pi_{\phi}(s_E), a_E)], \quad (1)$$

where \mathcal{D} is the dataset collected from the expert demonstration, s_E is the state experienced in \mathcal{D} , a_E is the expert's action in s_E , π_{ϕ} is the IL action policy parametrized by ϕ that we are training, and \mathcal{L} is the loss function. The action policy π_{ϕ} is trained to output actions similar to a_E for all s_E . However, due to the nature of supervised learning, π_{ϕ} can output actions similar to the expert actions only for the states or the similar states to those states included in the dataset. Therefore, when there is a shortage of expert data, or the data is immature, significant performance degradation is inevitable.

In contrast, RL is a technique where the agent interacts with the environment to develop an action policy that can maximize the cumulative rewards. It figures out appropriate actions to maximize the cumulative rewards on each state, based on its own experiences evaluated with the predefined reward function. The objective of RL is generally formulated as follows:

$$\max_{\phi} \mathbb{E}_{(s_t, a_t) \sim \rho_{\pi_{\phi}}} \left[\sum_{t=0}^{\infty} \gamma^t r(s_t, a_t) \right], \quad (2)$$

where π_{ϕ} is the RL action policy to be trained parametrized by ϕ , $\rho_{\pi_{\phi}}$ is the distribution of trajectory experienced by the agent using π_{ϕ} , $r(s_t, a_t)$ is the reward at time-step t , and γ is the discount factor.

Consequently, RL is trained to maximize the expectation of cumulative rewards obtained along an episode. Because RL experiences various episodes through extensive trial and error, it has the advantage of being robust in various situations compared to IL. However, as it needs to be trained through numerous interactions with random actions, it has low sample efficiency and slow training speed. Especially, the more complex the task, the broader the state space and action space, and the higher the transition variance, the more these problems are exacerbated, making it difficult to develop the optimal action policy or even initiate the training.

To complement the weaknesses of both IL and RL mentioned above, recent research on HL has focused on combining the two techniques. There are two main approaches to this fusion. The most representative approach is using pre-training and fine-tuning [18], [19], [21], [27], [28], where we initialize the weights of the policy network using IL (i.e., pre-training) and then fine-tunes the policy network using RL. Although this is the simplest approach, when the demonstration data for IL is immature, the action policy developed through IL can diverge significantly from the optimal policy pursued by RL. Consequently, during the fine-tuning process, the model weights may change drastically, potentially causing training instability, and making the pre-trained IL model ineffective.

Another approach combines the objectives of IL and RL so that demonstration data is considered together when training RL. A representative example is Behavior Cloned Soft

¹Over-correction causing the vehicle to skid more severely in the opposite direction.

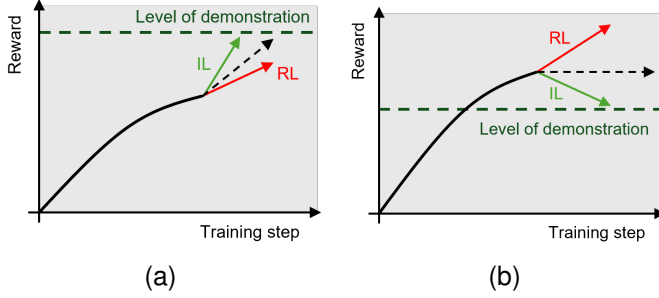


Fig. 3. Concept diagram. Impact of the quality of demonstration data on the training of action policy using existing HL techniques. (a) IL helps the training, when optimal demonstration data is given. (b) IL deteriorates the training, when immature demonstration data is given.

Actor-Critic (BC-SAC) [22], where the objective function of Behavior Cloning (BC) is added to the objective function of Soft Actor-Critic (SAC) [29] as:

$$\max_{\phi} \mathbb{E}_{(s,a) \sim \rho_{\pi_{\phi}}} [Q(s,a) + \alpha \mathcal{H}(\pi_{\phi}(\cdot|s))] + \lambda \cdot \mathbb{E}_{(s_E, a_E) \sim \mathcal{D}} [\log \pi_{\phi}(a_E|s_E)], \quad (3)$$

where $Q(s,a)$ is the action value function, \mathcal{H} is the entropy, α is the temperature, which is the weight of the entropy term, λ is the weight of the BC objective, and the first expectation term is the objective function of SAC. As described earlier, BC-SAC uses the demonstration data for RL rather than using a separate IL network trained with the demonstration data. Because of this, BC-SAC is robust even when the demonstration data is scarce, but the limitation is that the given demonstration must contain optimal data. Notice that the BC term, i.e., the second term in (3), tries to train the policy network to produce similar actions to the given demonstration, even if the demonstration is immature, while the SAC objective function directs the policy network to generate actions to maximize the cumulative reward. Therefore, when the given demonstration is noisy and does not contain optimal demonstration, these two objectives interfere each other and deteriorate the training process, as represented in Fig.3.

Such limitations in IL, RL, and HL become more critical in oversteer control and collision avoidance task. Firstly, it is nearly impossible to collect optimal demonstration data, because human drivers find it difficult to react appropriately and try immature vehicle control. As a result, the driving policy trained via IL or HL techniques could perform poorly. Moreover, there is an extensive amount of information to be perceived regarding the surroundings and the vehicle state, and there is a high transition variance due to the nonlinear dynamics. Not only does this make it challenging to develop an optimal driving policy using RL alone, but it also means that agents are unlikely to encounter the same situation multiple times, making it difficult to learn through repeated experiences. Therefore, there is a critical need for methods that enable fast learning from new situations and can rapidly incorporate new successful experiences into the learning process.

III. Q-VALUE COMPARED SOFT ACTOR-CRITIC (QC-SAC)

To address the aforementioned technical limitations of existing IL, RL, and HL techniques which are critical in developing an optimal driving policy capable of oversteer control and collision avoidance, we propose a novel HL technique called Q-Compared Soft Actor-Critic (QC-SAC). In this section, we introduce the three core elements of QC-SAC: Q-Compared Objective (QCO), Q-Network from Demonstration (QNfD), and Selective Demonstration Data Update (SDDU). QCO and QNfD contribute to the effective utilization of immature demonstration data to develop an optimal driving policy, while QNfD and SDDU facilitate the rapid incorporation of new successful experiences into the learning process.

A. Q-Compared Objective (QCO)

To effectively utilize immature demonstrations and support RL for optimal policy development with IL, QCO selectively utilizes only the beneficial demonstration data for behavior cloning (BC). It estimates the action value (Q) difference between the actions stored in the demonstration data and the actions generated by the driving policy being developed. Then, it prioritizes the demonstration data that have higher Q values than the driving policy being developed, where the prioritization is implemented by weighting the demonstration data in proportion to the quality difference. QCO thus resolves a critical problem in the conventional HL techniques; the action policy becomes suboptimal when immature demonstration data is provided.

QCO can be expressed as:

$$J_{\pi}(\phi) = J_{SAC}(\phi) + J_{BC}(\phi), \quad (4)$$

where the objective of the Soft Actor-Critic [30] RL is

$$J_{SAC}(\phi) = -\mathbb{E}_{(s,a) \sim \rho_{\pi_{\phi}}} [Q(s,a) + \alpha \mathcal{H}(\pi_{\phi}(\cdot|s))], \quad (5)$$

and objective of BC is

$$J_{BC}(\phi) = \mathbb{E}_{(s_d, a_d) \sim \mathcal{D}} [C(s_d, a_d) \cdot \mathcal{L}_1(a \sim \pi_{\phi}(s_d), a_d)]. \quad (6)$$

In (6), \mathcal{L}_1 represents the L₁ loss, and $C(s_d, a_d)$ is the Q-compared weighting factor for each demonstration data, which can be calculated as below.

$$C(s_d, a_d) = \max(Q^-(s_d, a_d) - Q(s_d, a \sim \pi_{\phi}(s_d)), 0), \quad (7)$$

where Q^- is the Q-target value.

The goal is to determine the parameters ϕ of the π network that minimize the cost function $J_{\pi}(\phi)$, which means that we determine ϕ that minimizes both the RL objective $J_{SAC}(\phi)$ (5) and the BC objective $J_{BC}(\phi)$ (6). Note that $J_{SAC}(\phi)$ (5) is the conventional SAC objective function, while $J_{BC}(\phi)$ (6) uses $C(s_d, a_d)$ for the Q value comparison. As shown in (7), $C(s_d, a_d)$ uses the action value function Q to evaluate which has the higher Q value between the given demonstration action

a_d and the action $a \sim \pi_\phi(s_d)$ of the RL action policy π_ϕ in the same state s_d . By multiplying the BC loss by the difference in two Q values as a weight, the more a_d has a higher Q value than $a \sim \pi_\phi(s_d)$, the more a_d is considered important and is given with higher priority. Additionally, by using the max function in (7), if a_d has a lower Q value than $a \sim \pi_\phi(s_d)$, a_d is considered to deteriorate the training and discarded from the training by setting the weight $C(s_d, a_d)$ to 0.

Additionally, to improve the numerical stability, L_1 loss is used for the BC loss in (6). As shown in (3), log probability can be used for BC when demonstration data is optimal. However, when a_d significantly differs from the distribution of $\pi_\phi(s_d)$ because of the immature demonstrations, $\pi_\phi(a_d|s_d)$ approaches to 0 and the log probability diverges. In contrast, L_1 loss is limited to the maximum value of 2 because of the action space constrained between -1 and 1, so that the risk of divergence is prevented. Since QC-SAC allows immature demonstrations, L_1 loss is used to ensure numerical stability even when immature demonstration data very different from $\pi_\phi(s_d)$ is given. In this manner, the QCO of QC-SAC is specialized for effective utilization of immature demonstrations.

B. Q-Network from Demonstration (QNfD)

Since Q values are used as the metric for evaluating a_d and $a \sim \pi_\phi(s_d)$ in (7), the Q-network must be well-trained to accurately estimate $C(s_d, a_d)$, thus enabling QCO to achieve high performance. Particularly in the oversteer control and collision avoidance task, where agents frequently encounter novel situations and have difficulties experiencing successful episodes due to broad state and action spaces and high transition variance, it is crucial to obtain as much data as possible to train the Q-network effectively. To achieve this, we propose QNfD method that utilizes demonstration data to enhance the Q-network training.

The concept of utilizing demonstration data for Q-network training is recently proposed, in the HL technique employing IL-based pre-training followed by fine-tuning with RL [31]. The study shows that when the RL is based on actor-critic, both networks for the actor and the critic need to be pre-trained. In our work, to fit the QC-SAC structure, which combines IL and RL into a single objective function without pre-training, we propose a method that combines two batches for the Q-network update. As expressed in lines 23~25 of Algorithm 1, the Q-network is updated using the union \mathcal{B} of the batch \mathcal{B}_{RL} sampled from the replay buffer \mathcal{D}_{RL} collected through interaction with the environment and the batch \mathcal{B}_{BC} sampled from the demonstration dataset \mathcal{D} . For this purpose, not only the state and action but also the reward and next state are recorded when collecting the demonstration data. The Q-network is updated using the following conventional objective function used in RL:

$$J_Q(\theta_i) = \mathbb{E}_{(s,a,r,s') \sim \pi} \left[\left(Q_{\theta_i}(s, a) - \hat{Q}(r, s') \right)^2 \right], \quad (8)$$

where Q_{θ_i} is parameterized by θ_i , $i \sim \{1, 2\}$ is the index of two Q-networks for double Q-learning [32], and

Algorithm 1 Q-value Compared Soft Actor-Critic (QC-SAC)

Require: demonstration dataset \mathcal{D} , average episode reward of demonstration \bar{r}_{epi} , discount factor γ , target update rate τ , target entropy $\bar{\mathcal{H}}$, and learning rates λ_Q , λ_π , λ_α

- 1: Initialize policy network π_ϕ and Q networks Q_{θ_1} , Q_{θ_2} with random weights
- 2: Initialize target Q-networks $Q_{\bar{\theta}_1}^-$, $Q_{\bar{\theta}_2}^-$ with weights $\bar{\theta}_1 \leftarrow \theta_1$, $\bar{\theta}_2 \leftarrow \theta_2$
- 3: Initialize entropy coefficient α
- 4: Initialize replay buffers $\mathcal{D}_{RL} \leftarrow \emptyset$, $\mathcal{D}_{epi} \leftarrow \emptyset$
- 5: Initialize episode reward $r_{epi} \leftarrow 0$
- 6: **for** each iteration **do**
- 7: **for** each environment step **do**
- 8: $a \sim \pi_\phi(a|s)$
- 9: $s' \sim p(s'|s, a)$
- 10: $\mathcal{D}_{RL} \leftarrow \mathcal{D}_{RL} \cup \{(s, a, r, s', d)\}$
- 11: $\mathcal{D}_{epi} \leftarrow \mathcal{D}_{epi} \cup \{(s, a, r, s', d)\}$
- 12: $r_{epi} \leftarrow r_{epi} + r$
- 13: **if** $d = 1$ **then**
- 14: **if** $r_{epi} > \bar{r}_{epi}$ **then**
- 15: $\mathcal{D} \leftarrow \mathcal{D} \cup \mathcal{D}_{epi}$
- 16: $\bar{r}_{epi} \leftarrow (\bar{r}_{epi} \cdot (|\mathcal{D}| - 1) + r_{epi}) / |\mathcal{D}|$
- 17: **end if**
- 18: $r_{epi} \leftarrow 0$
- 19: $\mathcal{D}_{epi} \leftarrow \emptyset$
- 20: **end if**
- 21: **end for**
- 22: **for** each gradient step **do**
- 23: Sample $\mathcal{B}_{RL} = \{(s, a, r, s', d)\}$ from \mathcal{D}_{RL}
- 24: Sample $\mathcal{B}_{BC} = \{(s_d, a_d, r_d, s'_d, d_d)\}$ from \mathcal{D}
- 25: Combined batch $\mathcal{B} = \mathcal{B}_{RL} \cup \mathcal{B}_{BC}$
- 26: $\theta_i \leftarrow \theta_i - \lambda_Q \nabla_{\theta_i} J_Q(\theta_i)$ for $i \in \{1, 2\}$ using \mathcal{B}
- 27: $\phi \leftarrow \phi - \lambda_\pi \nabla_\phi J_\pi(\phi)$ using $\mathcal{B}_{RL}, \mathcal{B}_{BC}$
- 28: $\alpha \leftarrow \alpha - \lambda_\alpha \nabla_\alpha J(\alpha, \bar{\mathcal{H}})$ using \mathcal{B}_{RL}
- 29: $\bar{\theta}_i \leftarrow \tau \theta_i + (1 - \tau) \bar{\theta}_i$ for $i \in \{1, 2\}$ using \mathcal{B}
- 30: **end for**
- 31: **end for**

$$\hat{Q}(r, s') = r + \gamma \mathbb{E}_{a' \sim \pi} [Q_{\bar{\theta}_i}^-(s', a') - \alpha \log \pi_\phi(a'|s')]. \quad (9)$$

Enhancing the performance of the Q-network through QNfD can significantly improve the performance of QC-SAC, i.e., it can produce more accurate Q value estimates for $C(s_d, a_d)$ and $J_{SAC}(\phi)$ (5) in QCO.

C. Selective Demonstration Data Update (SDDU)

In the oversteer control and collision avoidance task, where the state and action spaces are broad and the transition variance is high, agents often encounter novel situations and find it difficult to learn by experiencing the same situations multiple times. To address this challenge, we propose the SDDU method, which enables rapid learning from new situations and the swift incorporation of new successful experiences into the learning process. SDDU selects successful episodes from interactions with the environment during the training

process and uses aggregated data as the demonstration data for training. Before starting the training process, the average episode reward \bar{r}_{epi} of the demonstration data is recorded, which can be calculated as:

$$\bar{r}_{epi} = \frac{1}{|\mathcal{D}|} \sum_{i=1}^{|\mathcal{D}|} \sum_{j=1}^{|\mathcal{D}[i]|} r_{i,j}, \quad (10)$$

where $|\mathcal{D}|$ is the size of demonstration dataset \mathcal{D} , $|\mathcal{D}[i]|$ is the number of steps in the i^{th} episode in \mathcal{D} , and $r_{i,j}$ is the reward of the j^{th} step in the i^{th} episode.

Subsequently, while the agent interacts with the environment for training, at the end of each episode, the episode reward r_{epi} (i.e., the sum of reward received in that episode) is compared to \bar{r}_{epi} of the dataset. If the reward r_{epi} of the new episode is higher than \bar{r}_{epi} , the episode is added to the dataset, and \bar{r}_{epi} is updated again using (10). This iterative process is shown in lines 13~17 of Algorithm 1. By employing SDDU, the agent effectively expands its knowledge base with higher-quality data, enhancing the learning stability and performance of the driving policy. SDDU not only alleviates the data scarcity problem in IL by increasing the size and quality of the dataset, but also contributes to the effective minimization of QCO. After the iterative process of SDDU, we obtain the updated dataset \mathcal{D}' , which satisfies $\mathbb{E}_{(s,a) \sim \mathcal{D}'}[r(s,a)] > \mathbb{E}_{(s,a) \sim \mathcal{D}}[r(s,a)]$. Then, from $Q(s,a) = \mathbb{E}[\sum_{k=0}^{\infty} \gamma^k r_{t+k} | s_t = s, a_t = a]$, it follows that $\mathbb{E}_{(s,a) \sim \mathcal{D}'}[Q(s,a)] > \mathbb{E}_{(s,a) \sim \mathcal{D}}[Q(s,a)]$. Therefore, from (7), $\mathbb{E}_{(s,a) \sim \mathcal{D}'}[C(s,a)] > \mathbb{E}_{(s,a) \sim \mathcal{D}}[C(s,a)]$, and thus $J_{BC}(\phi)$ is considered more importantly, promoting active learning from expert behavior. Additionally, training π_ϕ by minimizing $J_{BC}(\phi)$ with \mathcal{D}' leads to higher $\mathbb{E}_{(s,a) \sim \rho_{\pi_\phi}}[Q(s,a)]$, contributing to the minimization of $J_{SAC}(\phi)$ as well.

In a summary, the proposed QC-SAC technique consists of three key elements: QCO, QNfD, and SDDU. The overall structure of QC-SAC can be found in Algorithm 1. We use (8) to update the Q-network and (4) to update the π network. The temperature α is updated using the same formula of the second version of SAC [30].

$$J(\alpha, \bar{\mathcal{H}}) = \mathbb{E}_{a \sim \pi} [-\alpha \log \pi(a|s) - \alpha \bar{\mathcal{H}}] \quad (11)$$

D. Focused Experience Replay (FER)

To improve training quality, we employ Focused Experience Replay (FER) [33]. FER addresses the data imbalance problem in conventional random sampling, where older data in the replay buffer is more likely to be sampled than recent data. By using a half-normal distribution for sampling, FER prioritizes recent data, enhancing training speed and stability.

IV. OVERSTEER CONTROL AND COLLISION AVOIDANCE BENCHMARK SETUP

A. Benchmark Setup

To develop the end-to-end driving policy network capable of oversteer control with collision avoidance, we propose a novel training and testing benchmark. The benchmark is inspired by the real driver training procedure which utilizes a kick plate: a

device that induces oversteer intentionally by moving laterally when the rear wheels of the vehicle pass over it. (see Fig.4a.) The human driver must control the oversteer while avoiding water fountains or virtual obstacles, as illustrated in Fig.4b. For safety reasons, we implement this within a simulator, creating a virtual kick plate to induce oversteer. Obstacles are then randomly placed on the road so that the autonomous vehicle encounters them after the oversteer is induced.

To compose the oversteer control and collision avoidance benchmark, a kick plate and obstacles are configured in the simulator. First, to deliberately induce oversteer, road friction is reduced by 50%, and a virtual kick plate is configured to apply lateral force to the rear tires as the vehicle passes a certain point. The lateral force applied to the rear tires is randomly set to vary the intensity and direction of the oversteer. Additionally, as shown in Fig.4c, obstacles are randomly placed within 30 to 70 m distance ahead of the kick plate. The distance between the kick plate and the obstacles is set closer than the legally recommended safe distance², rendering simple braking insufficient for collision avoidance and necessitating the formulation of precise avoidance trajectories. Furthermore, to prevent the cases where the road is entirely obstructed and driving becomes unfeasible, the number of obstacles placed is one fewer than the number of lanes. In the experiments, up to two obstacles are randomly positioned on a three-lane road.

B. State Space

The state space serving as input for RL and IL models is divided into two categories: vehicle state and surrounding state. The vehicle state includes eight values: side slip angle (β), longitudinal velocity (v_{long}), longitudinal acceleration (a_{long}), lateral acceleration (a_{lat}), cross-track error from original path or lane (d), orientation error with respect to original path (ψ), yaw rate ($\dot{\psi}$), and steering angle (δ). Side slip angle is calculated from v_{long} and lateral velocity (v_{lat}) ($\beta = \arctan\left(\frac{v_{lat}}{v_{long}}\right)$), while d and ψ are calculated based on the center line of the lane in which the vehicle was traveling before oversteering and the vehicle's center of gravity, respectively (see Fig.5a). The reason for considering the steering angle in the vehicle state will be discussed in the next section, with the action space setup. The surrounding state is composed of a 90-dimensional vector. This is a vectorized drivable area within a 90° azimuth range centered to front direction of the vehicle with 1° resolution, representing the drivable distance for each azimuth angle in polar coordinates. For each azimuth angle, the shortest distance to an obstacle or the road boundary is recorded. The visualization of the surrounding state vector can be seen in Fig.5b.

C. Action Space and Action Constraint

The action space is represented with a two-dimensional vector of pedal value and steering angular velocity. Generally,

²Converting the distance between the kick plate and the obstacles to Time to Collision (TTC) at an entry speed of 70 km/h, 30 m corresponds to 1.54 s, and 70 m corresponds to 3.60 s, which are within the legally defined safe distances. Generally, the safety distance required is 2 s in the US and Europe and 3.6 s in South Korea.

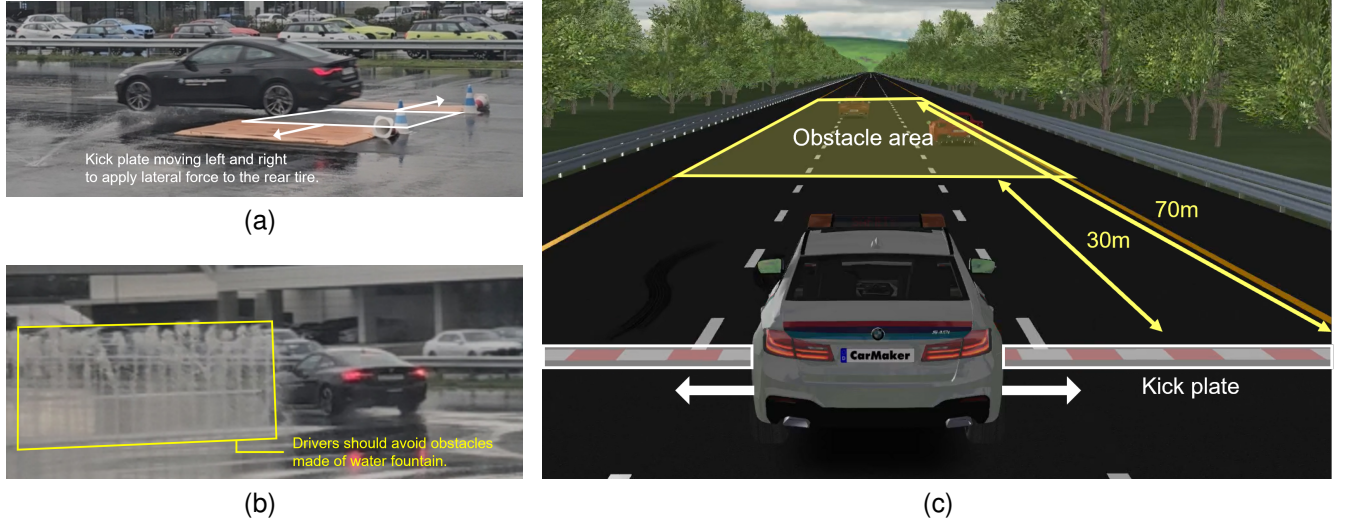


Fig. 4. Real-world driver training process and oversteer control and collision avoidance benchmark in a virtual environment. a, Kick plate inducing oversteer, and b, a collision avoidance scenario for driver training at BMW Driving Center, South Korea. c, Oversteer control and collision avoidance benchmark developed in IPG CarMaker simulator.

in end-to-end autonomous driving systems, the output action consists of longitudinal and lateral control values. For longitudinal control, it is typically either the target speed [21] or the pedal value [8], [9], [14], [28], while the lateral control value is usually the steering angle [8], [9], [14], [21], [28]. In the oversteer situation considered in this study, changes in weight transfer or slip ratio caused by pedal manipulation are more critical than the vehicle's speed. Therefore, the pedal value is selected as the longitudinal control value instead of the target speed. For lateral control, steering angular velocity is used instead of the steering angle to constrain the steering angular velocity. Note that when the steering angle is chosen as an action output, we cannot constrain the steering angular velocity, as the policy network can output very different steering angles at two consecutive time-steps. Indeed, when we develop a driving policy to produce the steering angle as an action, the maximum steering angular velocity records 18,000°/s. That means when the simulation runs at 20 Hz and the test vehicle has a steering range from -450° to 450° , a driving policy that steers with the maximum angular velocity is trained. An experiment video can be found at <https://youtu.be/BD4dNo4OM7k>. Since it is impractical to control the steering wheel in such a high angular velocity, we propose a method to constrain the vehicle's steering angular velocity. By specifying the steering angular velocity ($\dot{\delta}$) as an action output and considering the steering angle (δ) as part of the state, the steering angular velocity can be constrained without violating the Markov property. Considering the Markov property that the current state s_t is influenced only by the previous state s_{t-1} and the previous action a_{t-1} , and the definition that $\delta_{t-1} \in s_{t-1}$ and $\dot{\delta}_{t-1} \in a_{t-1}$, $\delta_t \in s_t$ can be expressed as $\delta_t = \delta_{t-1} + \dot{\delta}_{t-1} \cdot \Delta t$. Since time step Δt is fixed at 0.05 s in our 20 Hz simulation setup, our method does not violate the Markov property. In the simulation, both outputs, pedal value and steering angular velocity, are normalized between -1 and 1. Negative and positive pedal values indicate the brake and throttle pedal manipulations, respectively. The steering angular velocity is

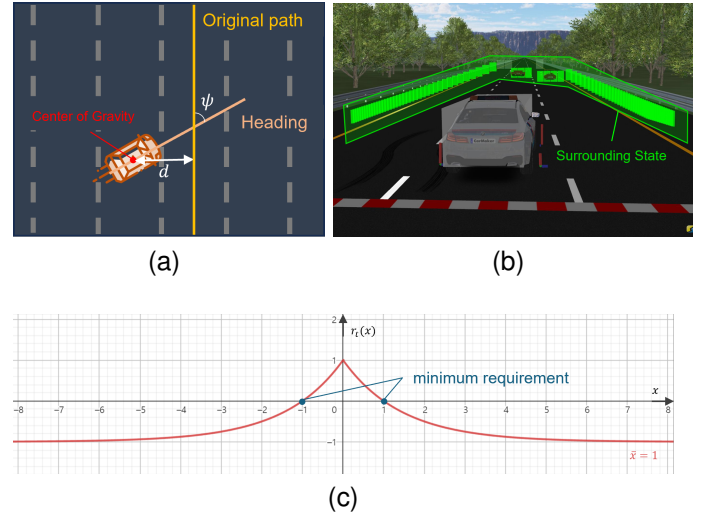


Fig. 5. Experimental setup. (a) Definition of d and ψ in vehicle state. (b) Representation of surrounding state. (c) An example of the reward function. ($\bar{x} = 1$).

set by multiplying the output value by 700°/s, ensuring that the maximum steering angular velocity is 700°/s. This value is based on the maximum steering angular velocity of the steer-by-wire system [34].

D. Reward Function Shaping

The reward function consists of four components: safe distance reward (R_{safe}), progress reward (R_{prog}), auxiliary reward (R_{aux}), and terminal reward (R_{term}). Except for R_{prog} and R_{term} , all reward functions adhere to the form of

$$r_t(x) = 0.5^{|x|/\bar{x}} \times 2 - 1, \quad (12)$$

where x is the value of interest, and \bar{x} is the predefined requirement value for x . This form of reward function is suitable for situations where a smaller x value is desired. It limits

the range of the reward value and considers the requirement value. Starting from an exponential function $r_t(x) = e^{-k|x|}$, it is modified to $r_t(x) = e^{-k|x|} \times 2 - 1$ to limit the reward value between -1 and 1. The x-intercept (at $x = -\frac{\ln(2)}{k}$) is set as the requirement value we aim to achieve at least. Aligning the x-intercept with the requirement value yields (12). The visualization of the reward function form is shown in Fig.5c.

Using the above function form in (12), each reward component considers the following variables as input x . For R_{safe} , the minimum value from the surrounding state information (drivable distance expressed in polar coordinates) is considered as the input. To maximize the safety distance from obstacles, -1 is multiplied when summing the total reward. For R_{aux} , the cross-track error, side slip angle, and steer rate are considered. We aim to minimize these values, in order to enhance passenger comfort, and improve control stability. Also, we strive to find an avoidance path that does not deviate significantly from the original path (i.e., the path planned before the oversteer) whenever possible.

Moreover, R_{prog} considers the distance traveled in the tangent direction within the Frenet-Serret frame, with respect to the path planned before the oversteer. The R_{prog} at time-step t is calculated as the difference in the distance traveled between time-steps t and $t-1$. Finally, R_{term} , added at the end of each episode, evaluates whether the episode was successful. When the side slip angle remains stable less than 1° for 100 time-steps, we consider that the vehicle is in the grip state, and the episode ends, granting a reward of +50. When the vehicle goes off-road, collides with an obstacle, or the side slip angle exceeds 37° (the vehicle's maximum wheel steer angle) and spins, a penalty of -50 is given.

The total reward (R_{tot}) that combines all four reward components is defined as follows:

$$R_{tot} = -\lambda_1 R_{safe} + \lambda_2 R_{prog} + \lambda_3 R_{aux} + R_{term}, \quad (13)$$

where λ_i for $i \in \{1, 2, 3\}$ is the weighting factor for each reward term.

In this study, we use weight values of $\lambda_1 = 0.8$, $\lambda_2 = 0.2$, $\lambda_3 = 0.2$. Additionally, the requirement values are set as follows: cross-track error to 3.5 m (the width of one lane), acceleration to 2.943 m/s^2 , side slip angle to 20° , and steer rate to $3000^\circ/\text{s}$.

V. PERFORMANCE EVALUATION

To evaluate the performance of QC-SAC, we compare the performance of driving policy developed with QC-SAC to those of three other representative conventional training techniques: Behavior Cloning (BC), Soft Actor-Critic (SAC) [30], and Behavior Cloned Soft Actor-Critic (BC-SAC) [22] that are representative and widely used IL, RL, and HL techniques, respectively. SAC is the most widely used RL technique for its strong performance, while BC-SAC is a representative HL technique that combines the objectives of BC and SAC. In this section, we demonstrate the superiority of QC-SAC by comparing the performance of driving policies in the proposed benchmark.

To develop a driving policy that can control oversteer and avoid nearby obstacles, we first build a dataset from demonstrations of a human driver with a racing wheel input device. A total of 25,567 time-steps, equivalent to 21.3 minutes of driving data, are collected from 200 episodes. Using the collected data, we develop driving policies using four techniques: BC, SAC, BC-SAC, and QC-SAC. The resulting reward graphs per training episode are shown in Fig.6a. Additionally, we infer the driving policies and conduct 500 episodes of test runs to compare the control & avoidance success rates of each approach. During the test runs, the location of obstacles and the intensity and direction of the oversteer induced by the kick plate are set completely random. The results are shown in TABLE I.

The reward graph and success rate of BC, which only learns from demonstration data without any interaction with the environment, testify the quality of the given demonstrations. As shown in Fig.6a, it is impossible to develop a good driving policy by solely using the given immature demonstration data. SAC, which maximizes rewards through the interaction with the environment, shows higher rewards than BC. However, as it is very difficult to experience successful episodes through random actions in the oversteer control and collision avoidance task, which has broad state and action spaces and high transition variance, SAC fails to develop the optimal driving policy. Note that selecting one wrong action in oversteer situation severely destabilizes the vehicle, making it impossible to complete the episode successfully. The probability that SAC consistently outputs appropriate actions at every time-step within an episode through random exploration is extremely low. BC-SAC, which considers both demonstration data and the interaction with the environment, performs slightly better than SAC but still cannot achieve high rewards as it continuously considers the immature demonstration data that disturbs the training.

In contrast, QC-SAC, which can effectively utilize immature demonstration data, records significantly higher rewards than other representative techniques. In the result of the test runs shown in Table I, the proposed technique records a control & avoidance success rate of about 81.8%. While this success rate might seem insufficient in the autonomous driving field, where safety is critical, it represents a significant improvement given the 34.6% success rate of existing techniques and the challenges human drivers encounter in the same situation. Indeed, human drivers who collected the dataset record about 15% success rate when conducting 100 test runs, when the positions of the front obstacles or the intensity and direction of the kick plate are unknown. Additionally, among the 91 episodes where QC-SAC fails to avoid collision, 95.6% (87 episodes) involve obstacles completely blocking the path in the direction of the vehicle's skid caused by the kick plate, making collision avoidance physically impossible within the given action space. Examples of these unavoidable collision failure cases can be seen in the video linked in Fig.7. Therefore, excluding unavoidable collisions, the driving policy developed via QC-SAC achieves a 99.0% success rate, demonstrating an almost optimal (i.e., near-optimal) performance.

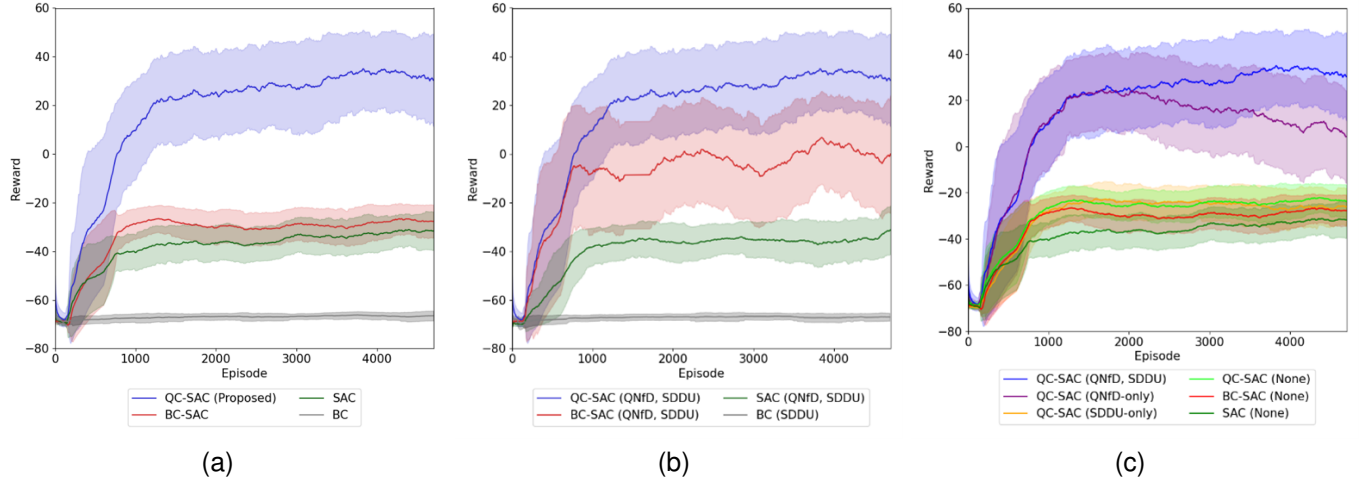


Fig. 6. Training curve. The solid line represents the average reward of five instances of each training technique initialized with random seeds, while the shaded area indicates their standard deviation. The proposed QC-SAC achieves significantly higher rewards compared to other techniques. (a) Performance evaluation, and (b,c) ablation study in the proposed benchmark. Because of the random obstacle placements, there are cases when the autonomous driving agent may not have any possible path to avoid the obstacles and the optimal policy inevitably experiences collisions. As a result, the standard deviation of the QC-SAC still remains high in the converged state.



Fig. 7. Captured scenes during the test runs. Videos of the test runs using QC-SAC in the oversteer control and collision avoidance benchmark can be found at <https://youtu.be/oflRob-hl6g>.

TABLE I
SUCCESS RATE FOR 500 EPISODES OF TEST RUNS.

Method	Success Rate	Success	Fail
QC-SAC (Proposed)	81.8%	409	91
BC-SAC [22]	34.6%	173	327
SAC [30]	19.0%	95	405
BC	0.0%	2	498

A. Ablation Study

An ablation study is conducted on the 3 core elements of QC-SAC (i.e., QCO, QNfD, and SDDU). First, to evaluate the impact of the objective function, QNfD and SDDU are applied to BC-SAC, SAC, and BC, under all other conditions to be the same except for the objective function. Note that QNfD is not applicable to BC because it does not use Q values for training. The comparison results are shown in Fig.6b. Compared to Fig.6a, it can be seen that the reward of BC-SAC and SAC slightly improves due to the application of

QNfD and SDDU, but still records significantly lower rewards compared to the proposed QC-SAC. This confirms that QCO is essential for developing an optimal action policy when immature demonstrations are given.

For the evaluation of QNfD and SDDU, we remove each function from the QC-SAC and observe the performance degradation. The results with SDDU and QNfD removed from the QC-SAC are labeled as QNfD-only and SDDU-only, respectively, while the results with both methods removed are labeled as None. As shown in Fig.6c, performance declines when SDDU and QNfD are not used, especially when QNfD is removed, there is a significant performance degradation. Because QC-SAC evaluates demonstration data based on Q values, when the performance of the Q-network decreases as the demonstration data is not used in Q-network training, the overall QC-SAC shows a substantial performance drop. This proves that QNfD is essential for QCO. On the other hand, when SDDU is discarded from QC-SAC, the reward graph starts to decline after around 2,000 episodes of training. This can be expected due to the overfitting from continuous behavior cloning on a fixed small set of demonstration data. Among the collected 25,567 time-steps of data, excluding those data with low Q values that are not considered by the QCO, a small amount of data could have been used for training, which causes an overfitting. In contrast, QC-SAC, which continuously updates and improves the demonstration data with successful episodes, does not encounter overfitting problem. Lastly, when both QNfD and SDDU are not implemented into QC-SAC, the performance of QC-SAC degrades significantly. However, due to the significant degradation by the removal of QNfD, the difference between None and QNfD-only is not substantial.

The results of the ablation study prove that all of the three core elements of QC-SAC, QCO, QNfD, and SDDU, are essential and critical. Therefore, the best performance is

achieved when all of these three elements are employed.

VI. CONCLUSION

In this study, we introduced an innovative autonomous driving technology capable of safely controlling oversteer while avoiding surrounding obstacles, achieved through the proposed Q-Compared Soft Actor-Critic (QC-SAC). Developing an optimal driving policy for oversteer control and collision avoidance is particularly challenging with existing IL, RL, and HL techniques due to RL's reliance on random exploration and IL and HL's dependence on nearly optimal expert demonstrations, which are difficult to obtain. QC-SAC addresses these challenges by effectively utilizing immature demonstration data and rapidly adapting to novel situations, making it a robust solution for developing optimal driving policies. We validated the superior performance of the driving policy trained via QC-SAC in the proposed benchmark inspired by real-world driver training procedures, significantly outperforming conventional techniques such as BC, SAC, and BC-SAC. Hence, this study proposes a pioneering autonomous driving technology that can significantly contribute to reducing accidents caused by oversteer.

ACKNOWLEDGMENTS

This work was supported by the National Research Foundation of Korea (NRF) grant funded by the Korea government (MSIT) (No. 2021R1A2C3008370). The authors thank IPG Automotive for providing CarMaker test licenses for the dissertation.

REFERENCES

- [1] P. Morton, *How to drift: The art of oversteer*. CarTech Inc, 2006.
- [2] A. Erke, "Effects of electronic stability control (esc) on accidents: A review of empirical evidence," *Accident Analysis & Prevention*, vol. 40, no. 1, pp. 167–173, 2008.
- [3] J. Y. Goh, T. Goel, and J. C. Gerdes, "A controller for automated drifting along complex trajectories," in *14th International Symposium on Advanced Vehicle Control (AVEC 2018)*, vol. 7, 2018, pp. 1–6.
- [4] E. Velenis, D. Katzourakis, E. Frazzoli, P. Tsiotras, and R. Happee, "Steady-state drifting stabilization of rwd vehicles," *Control Engineering Practice*, vol. 19, no. 11, pp. 1363–1376, 2011.
- [5] F. Zhang, J. Gonzales, S. E. Li, F. Borrelli, and K. Li, "Drift control for cornering maneuver of autonomous vehicles," *Mechatronics*, vol. 54, pp. 167–174, 2018.
- [6] I. Zubov, I. Afanasyev, A. Gabdullin, R. Mustafin, and I. Shimchik, "Autonomous drifting control in 3d car racing simulator," in *2018 International Conference on Intelligent Systems (IS)*. IEEE, 2018, pp. 235–241.
- [7] M. Acosta and S. Kanarachos, "Teaching a vehicle to autonomously drift: A data-based approach using neural networks," *Knowledge-Based Systems*, vol. 153, pp. 12–28, 2018.
- [8] P. Cai, X. Mei, L. Tai, Y. Sun, and M. Liu, "High-speed autonomous drifting with deep reinforcement learning," *IEEE Robotics and Automation Letters*, vol. 5, no. 2, pp. 1247–1254, 2020.
- [9] M. Cutler and J. P. How, "Autonomous drifting using simulation-aided reinforcement learning," in *2016 IEEE International Conference on Robotics and Automation (ICRA)*. IEEE, 2016, pp. 5442–5448.
- [10] P. S. Chib and P. Singh, "Recent advancements in end-to-end autonomous driving using deep learning: A survey," *IEEE Transactions on Intelligent Vehicles*, 2023.
- [11] L. Le Mero, D. Yi, M. Dianati, and A. Mouzakitis, "A survey on imitation learning techniques for end-to-end autonomous vehicles," *IEEE Transactions on Intelligent Transportation Systems*, vol. 23, no. 9, pp. 14 128–14 147, 2022.
- [12] Z. Zhu and H. Zhao, "A survey of deep rl and il for autonomous driving policy learning," *IEEE Transactions on Intelligent Transportation Systems*, vol. 23, no. 9, pp. 14 043–14 065, 2021.
- [13] B. R. Kiran, I. Sobh, V. Talpaert, P. Mannion, A. A. Al Sallab, S. Yogamani, and P. Pérez, "Deep reinforcement learning for autonomous driving: A survey," *IEEE Transactions on Intelligent Transportation Systems*, vol. 23, no. 6, pp. 4909–4926, 2021.
- [14] P. R. Wurman, S. Barrett, K. Kawamoto, J. MacGlashan, K. Subramanian, T. J. Walsh, R. Capobianco, A. Devlic, F. Eckert, F. Fuchs *et al.*, "Outracing champion gran turismo drivers with deep reinforcement learning," *Nature*, vol. 602, no. 7896, pp. 223–228, 2022.
- [15] E. Kaufmann, L. Bauersfeld, A. Loquercio, M. Müller, V. Koltun, and D. Scaramuzza, "Champion-level drone racing using deep reinforcement learning," *Nature*, vol. 620, no. 7976, pp. 982–987, 2023.
- [16] F. Huang, X. Deng, Y. He, and W. Jiang, "A novel policy based on action confidence limit to improve exploration efficiency in reinforcement learning," *Information Sciences*, vol. 640, p. 119011, 2023.
- [17] X. Zhao, "An empirical study of model-free exploration for deep reinforcement learning," Ph.D. dissertation, University of Alberta, 2021.
- [18] T. Hester, M. Vecerik, O. Pietquin, M. Lanctot, T. Schaul, B. Piot, D. Horgan, J. Quan, A. Sendonaris, I. Osband *et al.*, "Deep q-learning from demonstrations," in *Proceedings of the AAAI conference on artificial intelligence*, vol. 32, 2018.
- [19] A. Rajeswaran, V. Kumar, A. Gupta, G. Vezzani, J. Schulman, E. Todorov, and S. Levine, "Learning complex dexterous manipulation with deep reinforcement learning and demonstrations," *arXiv preprint arXiv:1709.10087*, 2017.
- [20] M. Alakuijala, G. Dulac-Arnold, J. Mairal, J. Ponce, and C. Schmid, "Residual reinforcement learning from demonstrations," *arXiv preprint arXiv:2106.08050*, 2021.
- [21] Y. Tian, X. Cao, K. Huang, C. Fei, Z. Zheng, and X. Ji, "Learning to drive like human beings: A method based on deep reinforcement learning," *IEEE Transactions on Intelligent Transportation Systems*, vol. 23, no. 7, pp. 6357–6367, 2021.
- [22] Y. Lu, J. Fu, G. Tucker, X. Pan, E. Bronstein, R. Roelofs, B. Sapp, B. White, A. Faust, S. Whiteson *et al.*, "Imitation is not enough: Robustifying imitation with reinforcement learning for challenging driving scenarios," in *2023 IEEE/RSJ International Conference on Intelligent Robots and Systems (IROS)*. IEEE, 2023, pp. 7553–7560.
- [23] Y. Gao, H. Xu, J. Lin, F. Yu, S. Levine, and T. Darrell, "Reinforcement learning from imperfect demonstrations," *arXiv preprint arXiv:1802.05313*, 2018.
- [24] W. Weng, C. Hu, Z. Li, H. Su, and L. Xie, "An aggressive cornering framework for autonomous vehicles combining trajectory planning and drift control," in *2024 IEEE Intelligent Vehicles Symposium (IV)*. IEEE, 2024, pp. 2749–2755.
- [25] H. B. Pacejka and E. Bakker, "The magic formula tyre model," *Vehicle system dynamics*, vol. 21, no. S1, pp. 1–18, 1992.
- [26] F. Braghin, F. Cheli, and E. Sabbioni, "Environmental effects on pacejka's scaling factors," *Vehicle System Dynamics*, vol. 44, no. 7, pp. 547–568, 2006.
- [27] P. Cai, H. Wang, H. Huang, Y. Liu, and M. Liu, "Vision-based autonomous car racing using deep imitative reinforcement learning," *IEEE Robotics and Automation Letters*, vol. 6, no. 4, pp. 7262–7269, 2021.
- [28] T. Wang and D. E. Chang, "Improved reinforcement learning through imitation learning pretraining towards image-based autonomous driving," in *2019 19th international conference on control, automation and systems (ICCAS)*. IEEE, 2019, pp. 1306–1310.
- [29] T. Haarnoja, A. Zhou, P. Abbeel, and S. Levine, "Soft actor-critic: Off-policy maximum entropy deep reinforcement learning with a stochastic actor," in *International conference on machine learning*. PMLR, 2018, pp. 1861–1870.
- [30] T. Haarnoja, A. Zhou, K. Hartikainen, G. Tucker, S. Ha, J. Tan, V. Kumar, H. Zhu, A. Gupta, P. Abbeel, and S. Levine, "Soft actor-critic algorithms and applications," 2019.
- [31] L. Wang, J. Liu, H. Shao, W. Wang, R. Chen, Y. Liu, and S. L. Waslander, "Efficient reinforcement learning for autonomous driving with parameterized skills and priors," *arXiv preprint arXiv:2305.04412*, 2023.
- [32] H. Hasselt, "Double q-learning," *Advances in neural information processing systems*, vol. 23, 2010.
- [33] S.-H. Kong, I. M. A. Nahrendra, and D.-H. Paek, "Enhanced off-policy reinforcement learning with focused experience replay," *IEEE Access*, vol. 9, pp. 93 152–93 164, 2021.
- [34] P. Yih and J. C. Gerdes, "Modification of vehicle handling characteristics via steer-by-wire," *IEEE transactions on control systems technology*, vol. 13, no. 6, pp. 965–976, 2005.



Seokjun Lee Seokjun Lee received a B.S. degree from the Department of Mechanical Engineering, Ulsan National Institute of Science and Technology (UNIST), Ulsan, South Korea, in 2023. He is currently enrolled in the Integrated M.S. and Ph.D. program at the Graduate School of Mobility, Korea Advanced Institute of Science and Technology (KAIST), Daejeon, South Korea. His research interests include end-to-end autonomous driving, autonomous driving on the handling limits, reinforcement learning and vehicle dynamics.



Seung-Hyun Kong (M'06–SM'16) is an Associate Professor in the CCS Graduate School of Mobility, Korea Advanced Institute of Science and Technology (KAIST), where he has been a faculty member since 2010. He received a B.S. degree in Electronics Engineering from Sogang University, Seoul, Korea, in 1992, an M.S. degree in Electrical and Computer Engineering from Polytechnic University (merged to NYU), New York, in 1994, and a Ph.D. degree in Aeronautics and Astronautics from Stanford University, Palo Alto, in 2005. From 1997 to 2004 and

from 2006 to 2010, he was with companies, including Samsung Electronics (Telecommunication Research Center) and Nexpilot, both in Korea, Polaris Wireless in San Jose, and Qualcomm (Corporate R&D) in San Diego, for advanced R&D in mobile communication systems, wireless positioning, and assisted GNSS. His current research interest includes deep neural networks for perception and localization using 4D Radar and sensor fusion, Reinforcement and Imitation learning algorithms for End-to-End autonomous driving, and neural network compression for embedded systems. He has authored more than 100 papers in peer-reviewed journals and conference proceedings and 14 patents, and his research group won the President's Award in the 2018 International Student Autonomous Driving Competition from the Korean government. He served as a Program co-Chair of IEEE ITSC 2019, New Zealand, and the General Chair of IEEE IV 2024, Korea, and he has served as an Associate Editor of IEEE T-ITS since 2017.